Supplementary figures and legends

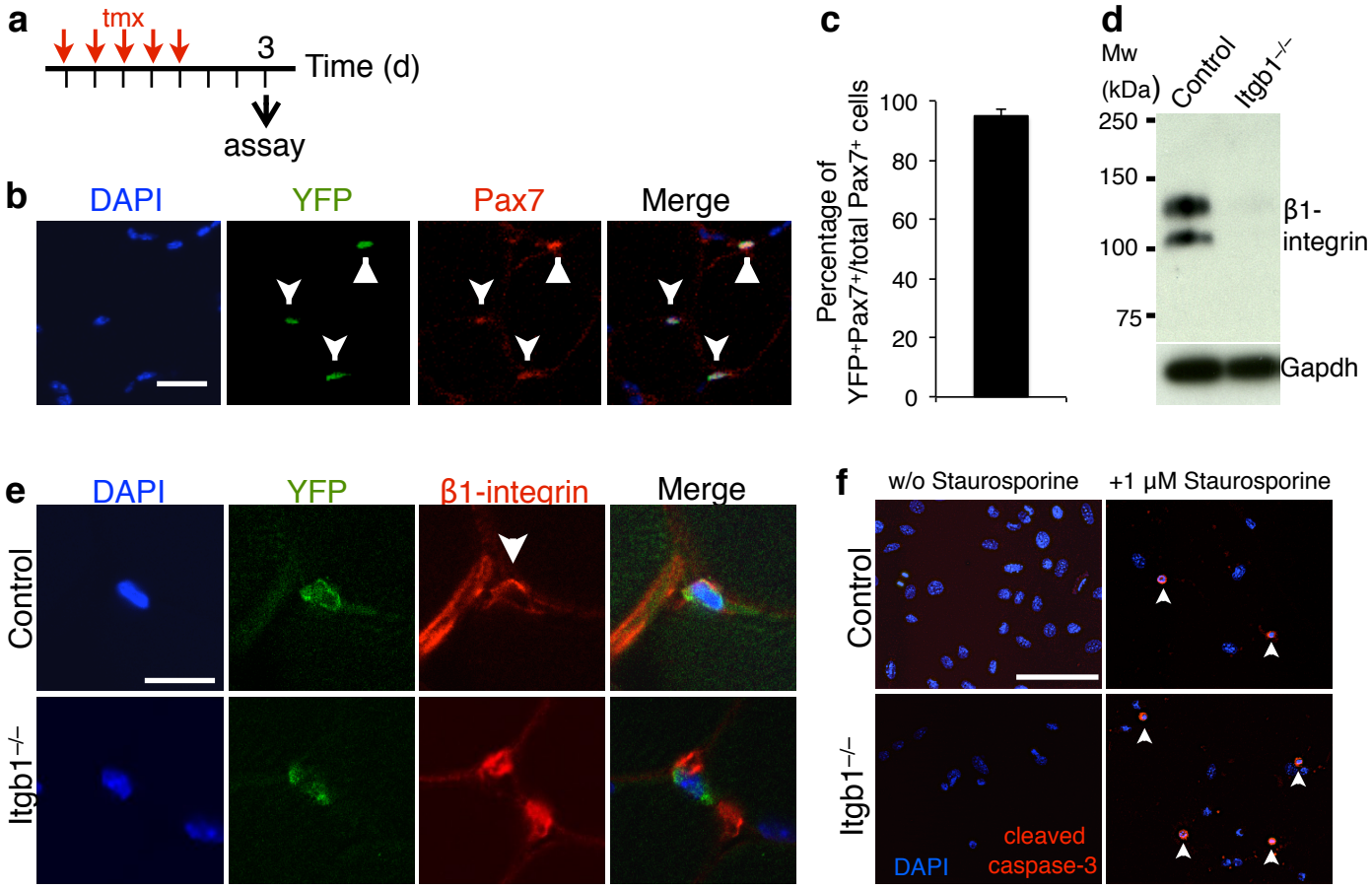

Supplementary Fig. 1: β1-integrin is specifically lost from Pax7⁺ SCs. (**a**) Tmx regimen and assay scheme for **Fig. 1a**; vertical lines indicate daily intervals. (**b**) SCs of control (*Pac7*$^{CE/+}$;*R26R*$^{YFP/YFP}$) animals stained for YFP and Pax7; arrowhead, YFP⁺Pax7⁺ SC; scale bar = 50 μm. (**c**) Percentage of YFP⁺Pax7⁺ in total Pax7⁺ SCs; *n* = 3 animals, ten sections per animal. Efficiency of tmx-induced YFP⁺ SC cell marking (95%) is comparable to that using the *R26R*^{LacZ} reporter[15]. (**d**) Western blot of FACS isolated control and *Itgb1*$^{-/-}$ YFP⁺ SCs (as in **Fig. 2c**). Two forms of β1-integrin in control are detected; the lower band is presumably β1D-integrin. Molecular weight (Mw, in kDa) is indicated. (**e**) YFP⁺ (arrows) control and *Itgb1*$^{-/-}$ SCs *in vivo* also show removal of β1-integrin in the mutant cell; scale bar = 20 μm. Due to antibody cross-reactivity, laminin staining is not provided here; it is presented in **Fig. 1a**. (**f**) Control and *Itgb1*$^{-/-}$ myoblasts in growth media for 3 d, then without or with 1 mM staurosporine treatment for 3 h, and probed for cleaved caspase-3 immune-reactivity for PCD; scale bar = 50 μm. Using this antibody *in vivo*, we did not find lineage marked mutant cells undergoing PCD. While we cannot formally exclude PCD as a partial mechanism for mutant SC reduction, we suggest it is not a major contributor.

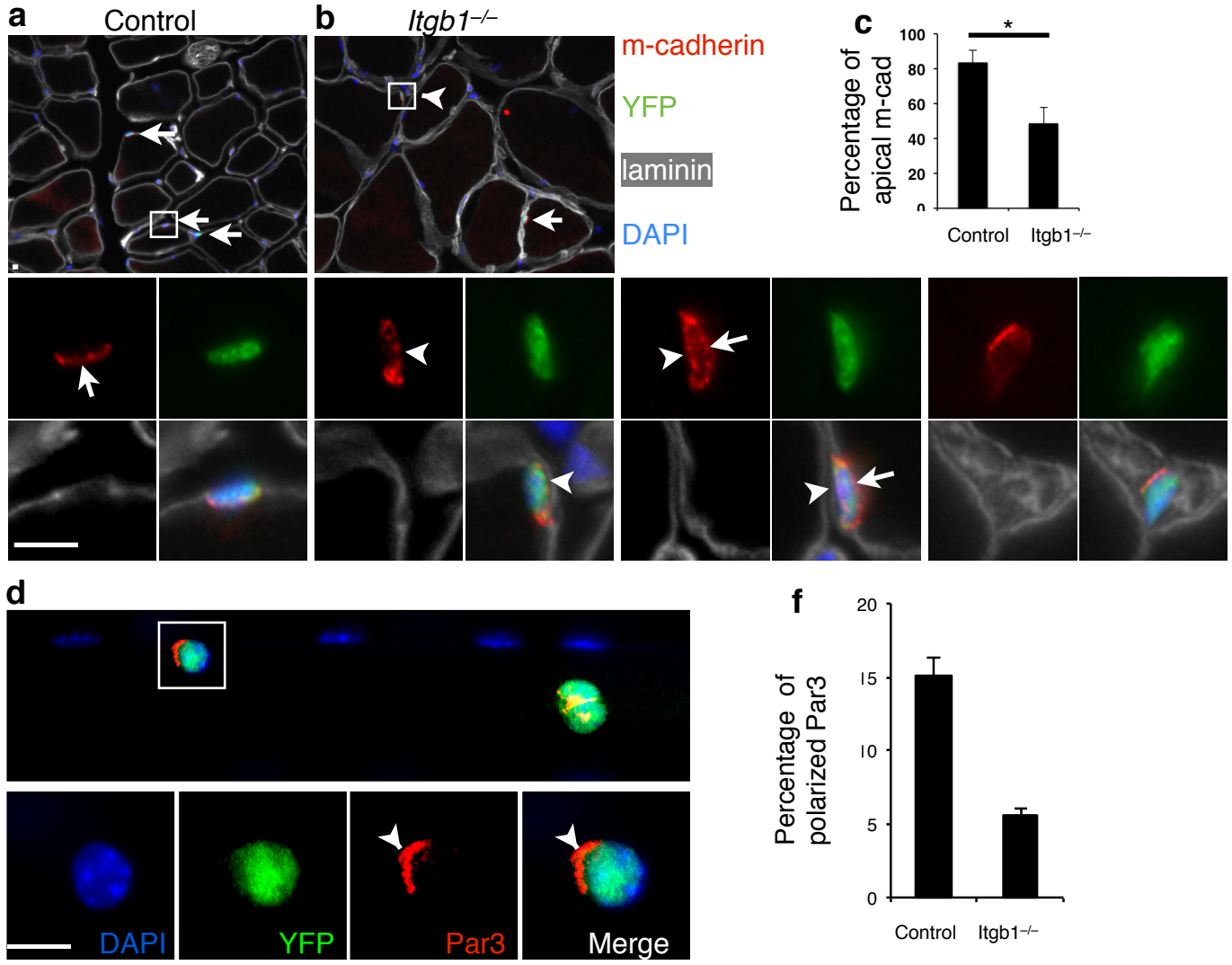

Supplementary Fig. 2: *Itgb1*$^{-/-}$ cells show defective polarity after 30 d. (**a-c**) M-cadhein is at the apical side (away from laminin) in YFP^{+} control (**a**), but abnormal in YFP^{+} *Itgb1*$^{-/-}$ cells (**b**) as quantified in (**c**); arrows, apical side; arrowhead, basal side. Enlarged images of the insets are below (**a**) and (**b**); additional examples of mutant cells are to the right; Scale bars, 5 μm. (**c**) Percent control and *Itgb1*$^{-/-}$ cells with apical m-cadeherin; n = 3 animals for each group, 5 sections per animal. (**d**) Two control SCs on myofiber stained for Par3, YFP and DAPI 30 h after isolation, show heterogeneity; enlarged images of the inset are below. (**e**) More examples of single control and mutant SCs stained as in (**d**); arrowheads, polarized Par3; Scale bars, 10 μm in (**d-e**). (**f**) Percent control and *Itgb1*$^{-/-}$ cells with polarized Par3. More than 20 fibers and 50 cells were scored for each group; Student's t-test: $^{*}P < 0.05$.

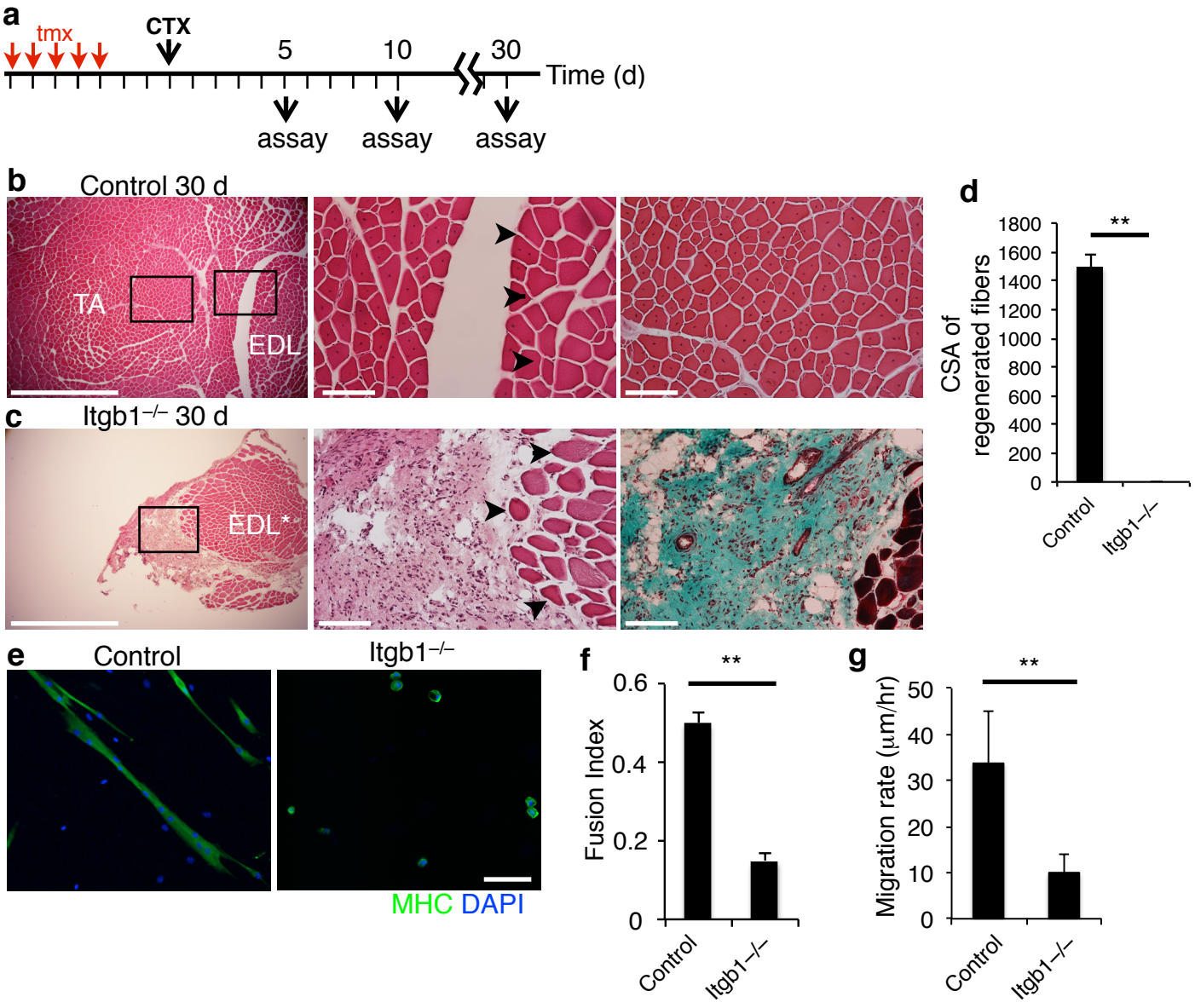

Supplementary Fig. 3: *Itgb1*$^{-/-}$ mice are defective in the entire muscle regeneration process. (**a**) The injury and regeneration assay scheme for **Fig. 1g-i**. (**b**) Control TA muscle at 30 d post injury by H&E stains at low (left) and high (right 2 images, boxed areas in the left image) magnifications; arrows indicate uninjured boundary. (**c**) Low (left) and high (middle, boxed area in the left image) magnifications of H&E stained *Itgb1*$^{-/-}$ muscle at 30 d after injury; arrows indicate the lack of central nuclei myofibers at the uninjured boundary. The right image is trichrome stain of a nearby section revealing extensive fibrosis (green area) next to uninjured muscle fibers (dark red). n = 3 for each group. Scale bars = 1 mm in left 2 images and = 100 μm in the high magnification images. **(d)** Cross sectional areas (CSA) of regenerated fibers of control and *Itgb1*$^{-/-}$ 30 d post injury. **(e-g)** *Itgb1*$^{-/-}$ cells are perpetuated by fusion and migration defects. (**e**, **f**) Control and *Itgb1*$^{-/-}$ YFP^{+} SCs were cultured in differentiation media for 3 d, and stained with MHC and DAPI in **(f)** to determine fusion index **(h)**; scale bar = 50 μm. **(g)** Control and *Itgb1*$^{-/-}$ myoblasts were monitored live to measure migration velocities; numerical data = mean ± s.d., n = 3 experiments; Student's t-test; $^{**}P < 0.01$.

a

Category	Number of differentially expressed genes	Number of up-regulated genes >2-fold	Percentage
0hr	0	——	——
24hr	0	——	——
48hr	252	15	5.95%
72hr	627	304	48.48%

b

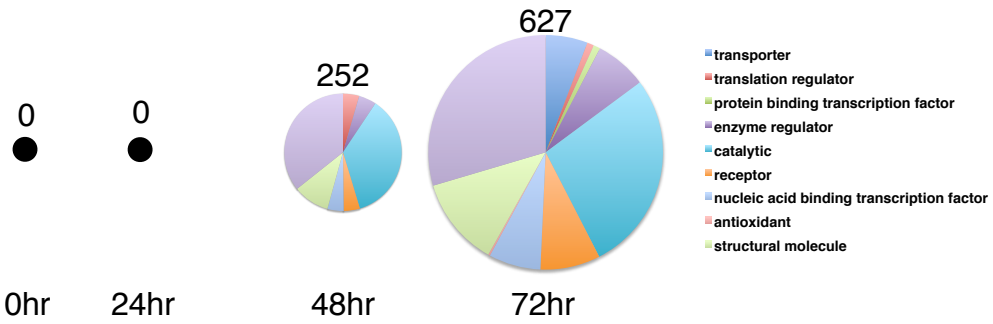

c

Upregulated	gene	control fpkm	itgb1 fpkm	log2(fold_change)	test_stat	p_value	q_value	significant
1	**Ckm**	0	12.606	1.79769E+308	1.79769E+308	0.00034093	0.013169	yes
2	**Prss46**	0.0059601	6.20581	10.0241	-3.79457	0.00014789	0.00692066	yes
3	**Cox8b**	0.041635	34.0536	9.67579	-3.6481	0.00026419	0.0108326	yes
4	**Mfap4**	0.0143559	7.51532	9.03205	-3.89013	0.00010019	0.00513513	yes
5	**Hrc**	0.0316929	9.26835	8.19201	-5.08914	3.60E-07	5.18E-05	yes
6	**Slc5a5**	0.0269844	6.5643	7.92637	-4.54134	5.59E-06	0.000513728	yes
7	**Dbh**	0.0380671	6.96503	7.51544	-4.85841	1.18E-06	0.000132511	yes
8	**Mb**	0.767165	137.154	7.48204	-6.40189	1.53E-10	5.38E-08	yes
9	**Trim72**	0.046796	5.87931	6.97312	-3.87861	0.00010505	0.00534327	yes
10	**Csrp3**	0.351137	35.6742	6.6667	-4.35297	1.34E-05	0.00101624	yes
Downregulated	gene	control fpkm	itgb1 fpkm	log2(fold_change)	test_stat	p_value	q_value	significant
1	**U90926**	14.8419	0.23332	-5.99122	3.90069	9.59E-05	0.00495426	yes
2	**AA467197**	17.842	0.529519	-5.07445	3.46471	0.00053080	0.0180448	yes
3	**Basp1**	16.7405	0.65291	-4.68031	4.6894	2.74E-06	0.000278731	yes
4	**Gm12603**	16.8879	0.751285	-4.49048	3.96189	7.44E-05	0.00407537	yes
5	**Rpl35**	499.626	35.6063	-3.81065	7.08494	1.39E-12	6.39E-10	yes
6	**Nrcam**	5.73605	0.448023	-3.67841	5.59399	2.22E-08	4.93E-06	yes
7	**Tubb3**	6.96417	0.545219	-3.67504	3.33631	0.00084899	0.0250857	yes
8	**Fabp5**	40.2442	3.1561	-3.67256	5.0851	3.67E-07	5.18E-05	yes
9	**Psmb10**	10.7249	1.04097	-3.36496	3.21931	0.001285	0.0339227	yes
10	**Peg10**	30.1804	3.26443	-3.20871	7.75165	9.10E-15	6.07E-12	yes

Supplementary Fig. 4: **RNA-seq data reveal that *Itgb1*$^{-/-}$ SCs display gene expression changes progressively over 72 h.** Tables (**a, c**) and pie charts (**b**) summarize results from RNA-seq analyses for **Fig. 2g**, comparing gene expression changes in mutant vs. control cells after culture in 10% horse serum growth media for 24, 48, and 72 h. (**a)** Differentially expressed genes were determined by Cuffdiff 2 to have significant q-values. (**b**) Schematic representation of (**a**). Functional categories provided by PANTHER. Similar gene categories represented between 48 and 72 h, although in different numbers. Pathway analyses did not uncover significant changes in relevant signaling pathways. (**c**) Top 10 Upregulated and Downregulated genes as determined by Cuffdiff 2, an algorithm that estimates expression at transcript-level resolution and controls for variability evident across replicate libraries. Genes were included only if one (control or Itgb1) had FPKM ≥ 5 to control for elevated fold changes of genes with minimal expression.

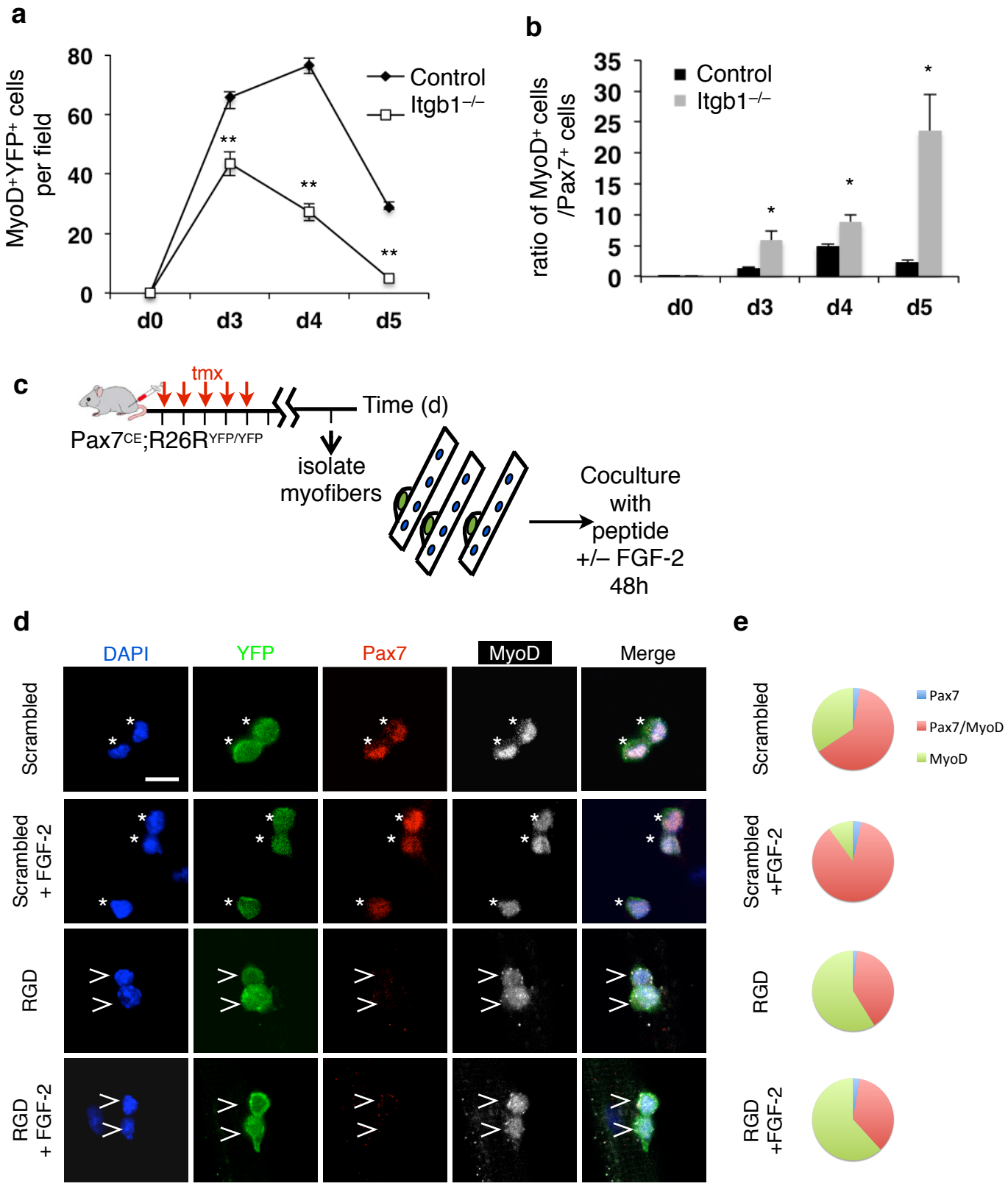
a
MyoD+YFP+ cells per field
80
60
40
20
0
Control
Itgb1−/−
**
**
**
d0
d3
d4
d5
b
ratio of MyoD+ cells /Pax7+ cells
35
30
25
20
15
10
5
0
Control
Itgb1−/−
*
*
*
d0
d3
d4
d5
c
tmx
Pax7CE;R26RYFP/YFP
Time (d)
isolate myofibers
Coculture with peptide +/– FGF-2 48h
d
DAPI
YFP
Pax7
MyoD
Merge
Scrambled
Scrambled + FGF-2
RGD
RGD + FGF-2
e
Scrambled
Scrambled +FGF-2
RGD
RGD +FGF-2
Pax7
Pax7/MyoD
MyoD

Supplementary Fig. 5: *Itgb1*$^{-/-}$ SCs and control SCs treated with RGD peptide are prone to differentiation. (a, b) are support data for **Fig. 2a**: (**a**) Average number of MyoD^{+}YFP^{+} cells per field (0.228 μm^2) from the same samples in **Fig. 2a** through the course of regeneration. (**b**) Ratios of MyoD^{+} versus Pax7^{+} cells (in **Fig. 2b**). Data are expressed as mean ± s.e.m; Student's *t*-test: **P* < 0.05; ***P* < 0.01; *n* = 3 animals per time point, 10 sections scored per animal**.** (**c**) Myofiber-associated control young YFP^{+} SCs of were cultured for 48 h with scrambled or RGD peptide and with or without FGF-2 and stained for Pax7 and MyoD. (**d**) SCs are self-renewed (Pax7^{+}MyoD^{-}), proliferating and self-renewable (Pax7^{+}MyoD^{+}; asterisk), or committed to differentiation (Pax7^{-}MyoD^{+}; open arrowhead); confocal images; scale bar = 10 μm. (**e**) Pie charts summarize data in (**a**); *n* ≥ 25 myofibers per condition; two-way ANOVA was used for paired comparison: *P* < 0.05, scrambled vs. scrambled + FGF-2 for Pax7^{-} MyoD^{+} and scrambled vs. RGD + FGF-2; not significant, RGD vs. RGD + FGF-2 for Pax7^{-}MyoD^{+}. RGD-peptide treatment caused SCs to fall off the myofiber over time, and therefore shorter time frame was used. In this context, there were very few Pax7^{+}MyoD^{-} cells. Our conclusion is based on Pax7^{+}MyoD^{+} fractions, as these cells have the potential to self-renew by turning off MyoD.

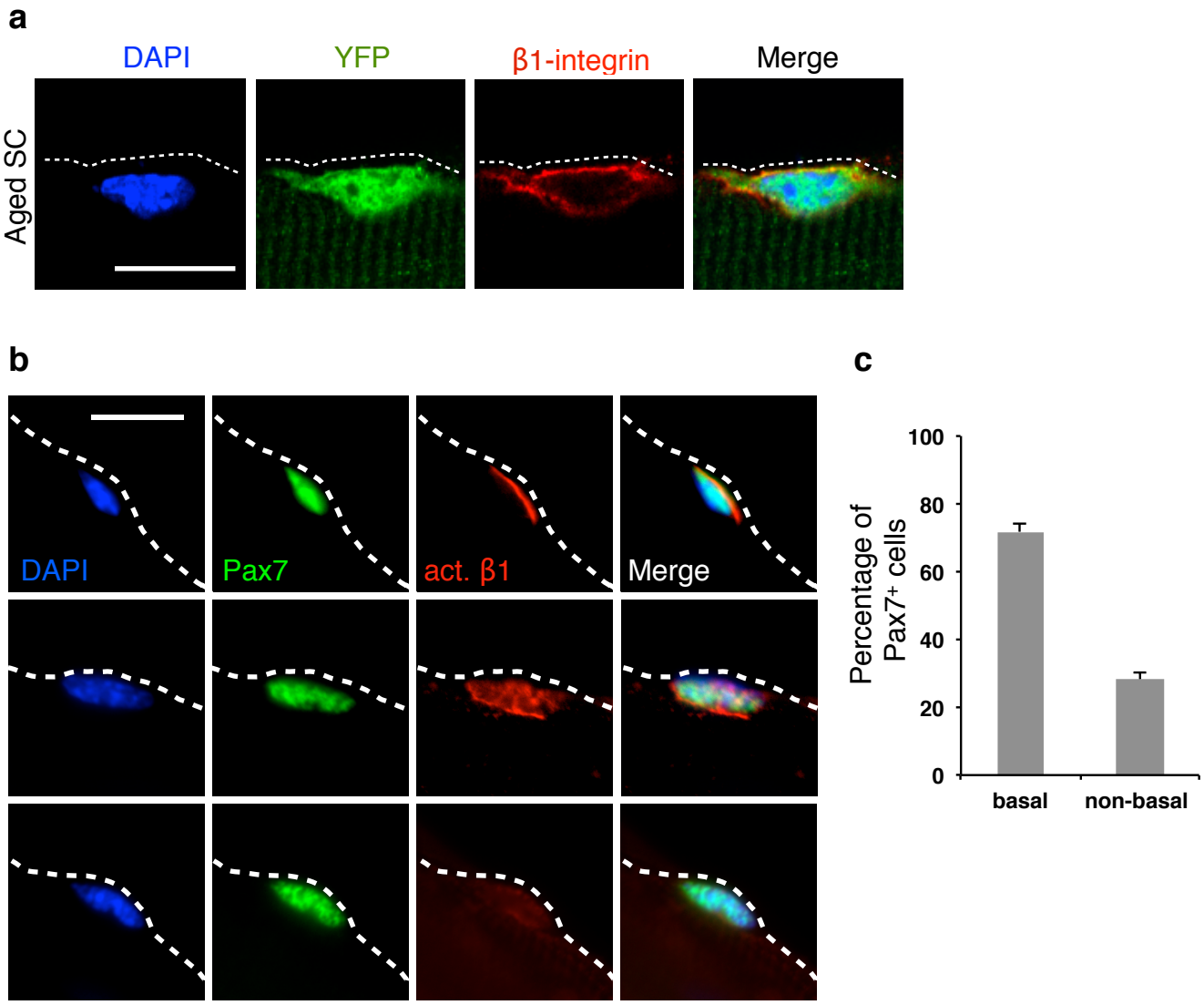

Supplementary Fig. 6: Distribution of β1-integrin in aged and dystrophic SCs. (a) Aged SCs show laminar-localized pan β1-integrin. YFP$^+$ myofiber-associated SCs of aged mice at 1 h after isolation stained for pan β1-integrin. Localization pattern mirrors young control SCs stained for pan-β1 integrin (**Fig. 1a**); dashed lines outline the basal side of the myofiber; scale bar = 10 μm. **(b, c)** SCs on *mdx* myofibers have dysregulated β1-integrin activity: **(b)** Pax7$^+$ SCs on myofibers after isolation from *mdx* mice show basally restricted (top) and non-basally restricted (middle and bottom) activated β1-integrin (act. β1) patterns (same exposure time), compared to control (**Fig. 4a**, **b**, young SC). **(c)** Percentages of act. β1 displaying basal and non-basal pattern in the Pax7$^+$ SC population.

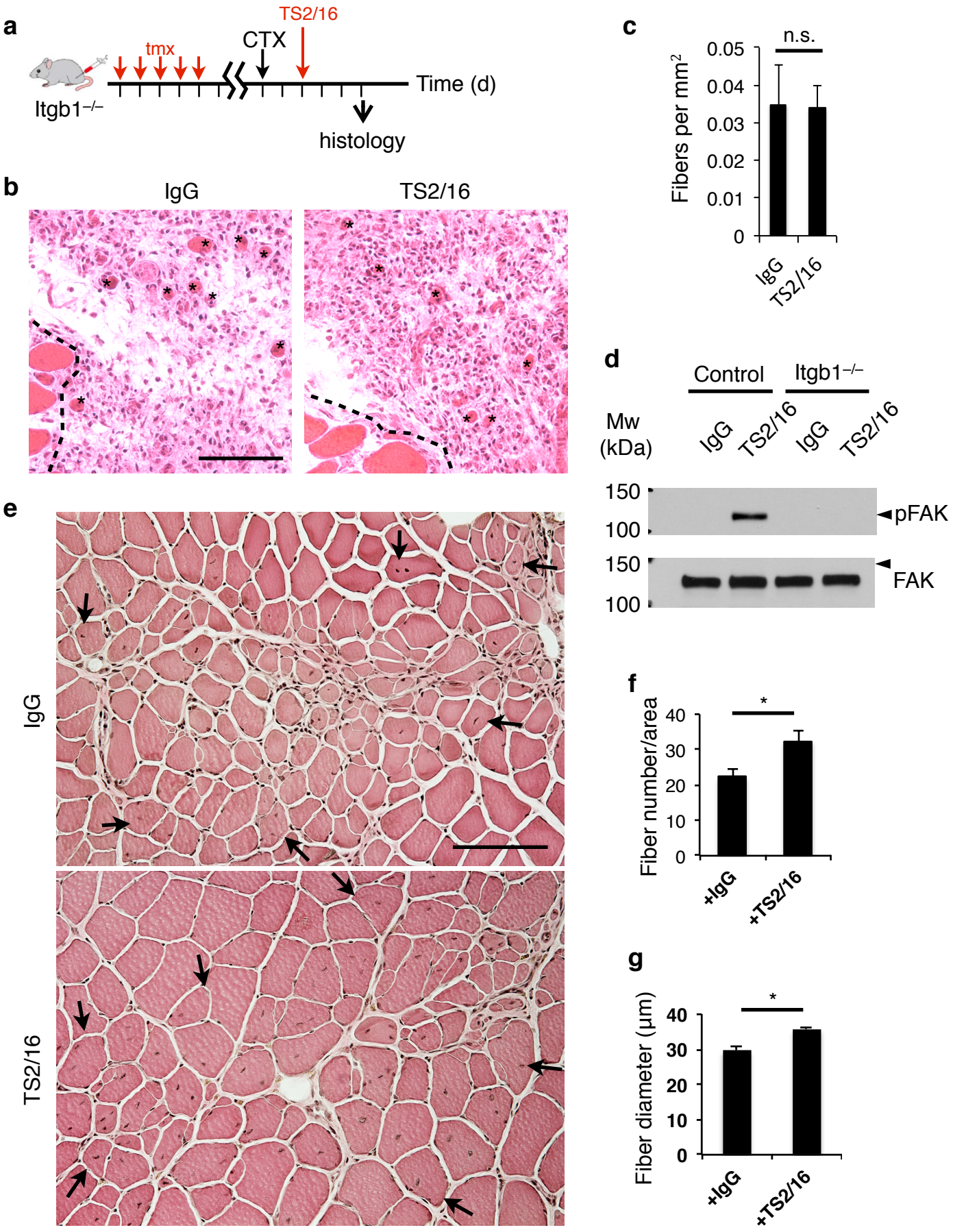
a
TS2/16
tmx
CTX
Time (d)
Itgb1−/−
histology
b
IgG
TS2/16
c
n.s.
Fibers per mm2
0.05
0.04
0.03
0.02
0.01
0
IgG
TS2/16
d
Control
Itgb1−/−
Mw
(kDa)
IgG
TS2/16
IgG
TS2/16
150
100
pFAK
150
100
FAK
e
IgG
TS2/16
f
Fiber number/area
40
30
20
10
0
*
+IgG
+TS2/16
g
Fiber diameter (µm)
40
30
20
10
0
*
+IgG
+TS2/16

Supplementary Fig. 7: TS2/16 specifically activates β1-integrin and support long-term muscle regeneration: (a-c) TS2/16 does not rescue the regeneration deficiency of *Itgb1*$^{-/-}$ muscle: **(a)** Tmx regimen, CTX injury, and TS2/16 injection scheme. 2 - 4 d post injury, 6 × 10 μl injections into the injury site of either vehicle IgG or TS2/16 (10 μg/ml). (**b**) TA muscles were harvested at 5 d post injury, and cross-sections were H&E stained; scale bar = 150 μm. (**c**) Regeneration was quantified by central nuclei myofibers in the injured area. Data represent mean ± s.e.m.; $n = 3$ animals per condition; ten sections per animal; one-way ANOVA: n.s., not significant. **(d)** TS2/16 activates FAK phosphorylation (pFAK) in control but not *Itgb1*$^{-/-}$ myoblasts. **(e-g)** TS2/16-enhanced aged muscle regeneration persists to 30 d post injury: (**e**) Representative images for IgG-treated (top) and TS2/16-treated (bottom) aged muscle sections 30 d after needle-track injury; arrows indicate boundaries of regenerative tracks; n = 4 animals for each group; scale bar = 100 μm. (**f, g**) Average number of fibers (**f**) with centrally located nuclei per regenerative area (0.216 mm^2) and average fiber diameters **(g)** of each group are presented as mean ± sem; Student's *t* test: $*P < 0.05$.

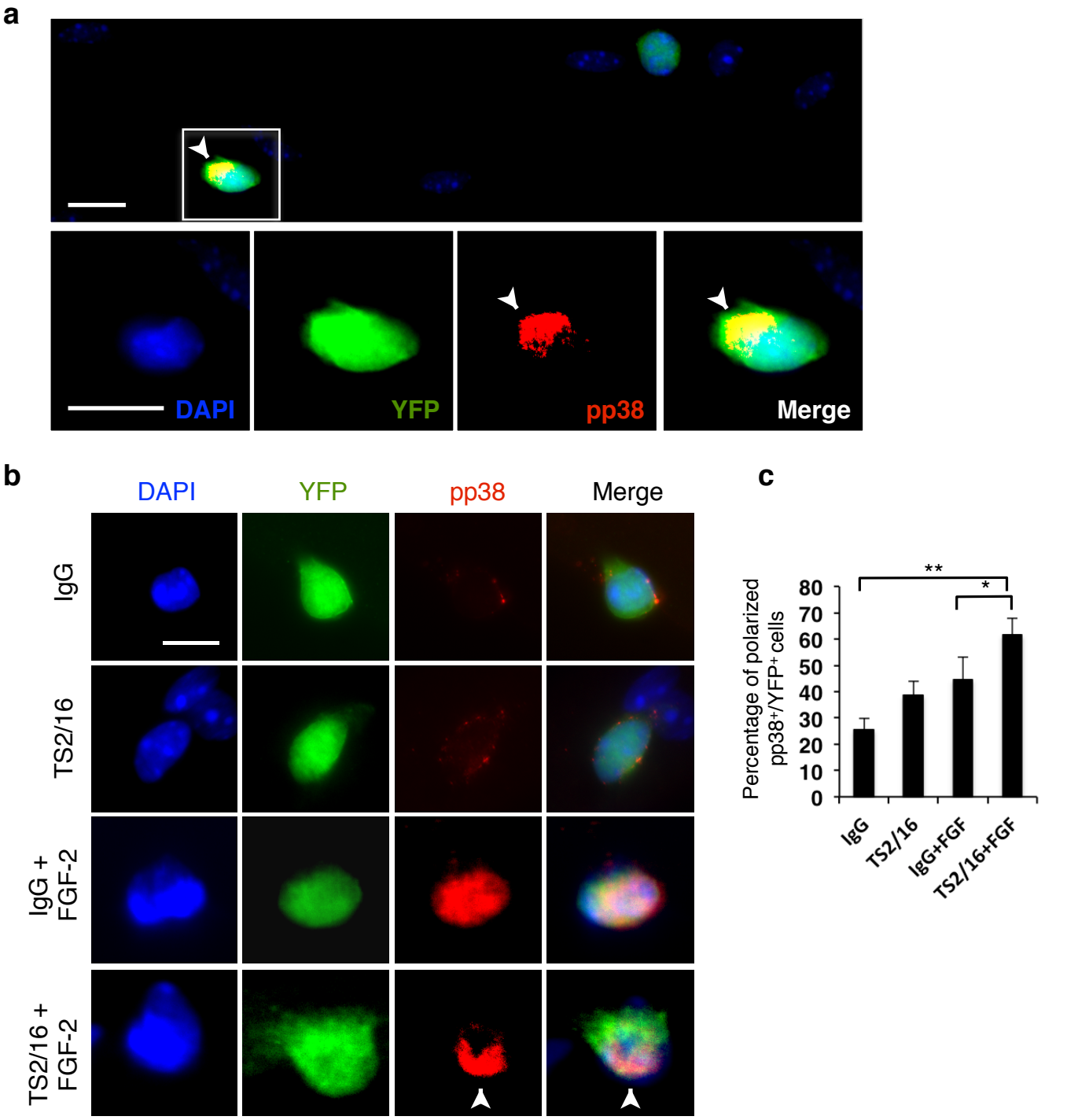

Supplementary Fig. 8: TS2/16 and FGF-2 increase the fraction of aged SCs displaying polarized pp38. **(a)** Two cells on a single myofiber show heterogeneity of pp38 staining between YFP-marked SCs for **Fig. 2g**. The cell in the inset shows polarized pp38, while the other shows none-to-minimal pp38 signal; scale bars = 10 μm. **(b)** Additional single cell examples of various patterns of pp38 distribution in aged myofiber-associated lineage-marked YFP+ SCs cultured for 30 h with control IgG or TS2/16 (10 μg/ml), with or without FGF-2 (10 ng/ml); scale bar = 10 μm. **(c)** Percentages of SCs with polarized pp38 (arrowhead in **a** and **b**); those with only a few puncta of pp38 signal were not counted as polarized; n = 3 experimental replicates, ≥ 25 myofibers each condition per replicate; Student's t-test paired comparison: $^{*}P < 0.05$, $^{**}P < 0.01$.

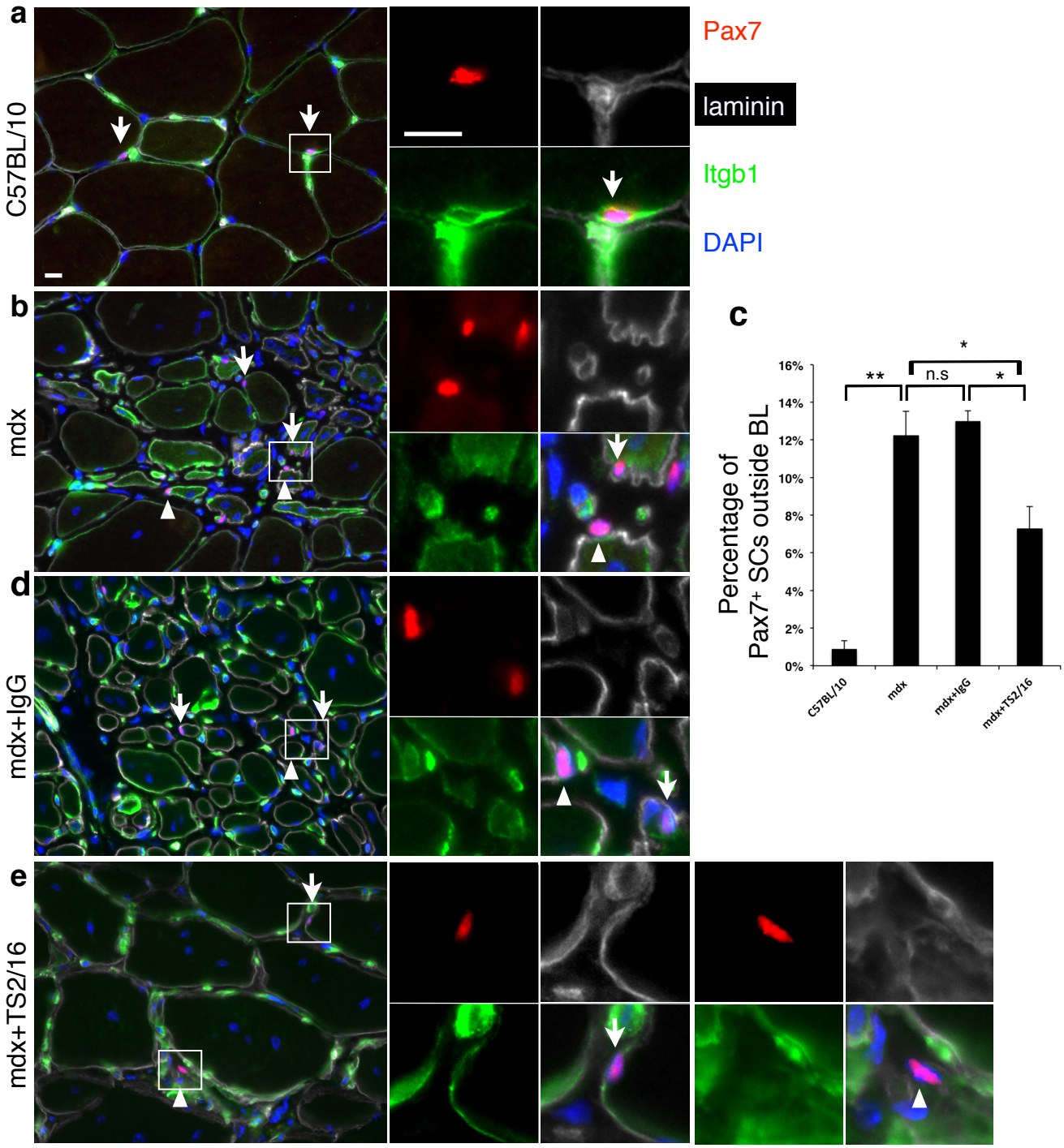

Supplementary Fig. 9: TS2/16-treated *mdx* mice have reduced fraction of SCs outside the myofiber basal lamina. (**a**) control C57/BL10 and (**b**) *mdx* TA muscles stained for Pax7, laminin, pan-β1-integrin, and DAPI; arrows, Pax7+ SCs inside the myofiber laminin basal lamina (BL); arrowheads, Pax7+ SCs outside the BL. (**c**) Percentages of Pax7+ SCs outside the BL for all groups in (**a**, **b**, **d**, and **e**); n = 3 animals per group; > 100 SCs counted per group; Student's *t*-test, paired comparison: $*P < 0.05$, $**P < 0.01$, and n.s., not significant. (**d**) IgG-treated *mdx* and (**e**) TS2/16-treated *mdx* TA muscles stained and labeled as (**a**) and (**b**), and quantified in (**c**). Enlarged images for each inset in (**a**, **b**, **d**, and **e**) are to the left. (**e**) has two insets; images for the top inset is to the immediate right, and for the bottom inset, further right. Scale bars, 10 μm.

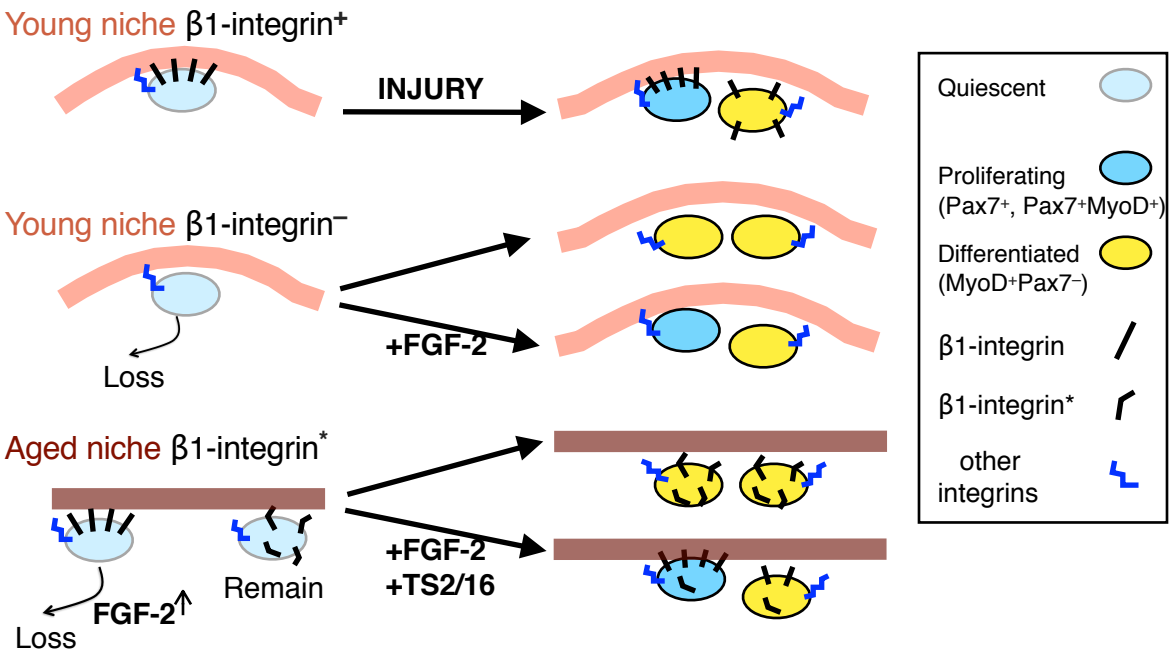

Supplemental Fig. 10: Models for β1-integrin function in young and aged SC niches. Keys to the symbols are to the right. **Top panel:** Young SCs uses β1-integrin to sense and occupy the quiescent niche, and they can support injury-induced expansion and renewal. **Middle panel:** β1-integrin mutant young SCs are prone to loss, and cannot support injury-induced expansion and renewal. FGF-2 partially rescues these defects in vitro, but unlikely to rescue the fusion defect to support regeneration in vivo. **Bottom panel:** During the aging process, SCs with sufficient overall integrin activity cooperate with increasing levels of FGF-2, break quiescence, and become lost. The remaining aged SCs with integrin dystruglation, reflected by abnormal patterns of active β1-integrin (β1-integrin*), are non-responsive to FGF-2, but can be rescued by TS2/16 and FGF-2.